



# Mapping the Sun's active regions from SDO images to HARPS-N solar spectra

This Work is Submitted for the Astrophysics Laboratory II class by:

Mariana Carolina Villamil Sastre

Université de Genève  
Faculty of Science  
Astronomy Department

Advisor  
**Michael Cretiginier. Ph.D**

Geneva, Switzerland  
2022

# **Mapping the Sun's active regions from SDO images to HARPS-N solar spectra**

Mariana Carolina Villamil Sastre

Université de Genève

## **Abstract**

Active regions are the main observable of magnetic activity in the Sun, these zones include structures such as faculae, sunspots and plage, the first two are located at the photosphere and the third one at the chromosphere, respectively. The aim of this work was to perform an analysis to determine if there's any individual contribution to the relative spectra driven by Sun's activity. Besides that, correlate the disc-integrated spectra (HARPS-N) with the spot and plage filling factors measured with images taken by the Solar Dynamics Observatory (SDO). Using a previous code (YAMORI, Cretignier et. al in prep), we found that there's no clear evidence of sensitivity to sunspot-faculae activity due to an interference pattern and systematics from the detector. Nevertheless, an equivalent of a stellar surface-tomography analysis was performed during the process and it was possible to observe strong features in spectral lines affected by plage and spot at the same time.

# Contents

<b>1 Objectives</b>	<b>3</b>
1.1 General Objective . . . . .	3
1.2 Specific Objectives . . . . .	3
<b>2 Introduction</b>	<b>4</b>
2.1 HARPS-N . . . . .	6
2.2 SDO Images . . . . .	7
<b>3 Methodology</b>	<b>8</b>
3.1 Left-Right area method . . . . .	11
<b>4 Results</b>	<b>14</b>
<b>5 Conclusions</b>	<b>18</b>

# Chapter 1

## Objectives

### 1.1 General Objective

Map a disk-integrated spectra obtained by HARPS-N with solar direct images (SDO) in the UV filter.

### 1.2 Specific Objectives

- Identify the occurrence of Sun's active regions with SDO images.
- Measure the effect that activity and rotating active regions can have on the measurement of spectral lines.
- Disentangle the contributions from different active regions.

# Chapter 2

## Introduction

Active regions are the primary observable of magnetic activity in the Sun, these zones include structures such as **faculae**, **sunspots** and **plage**, the first two are located at the photosphere and the third one at the chromosphere, respectively. Sunspots are described as zones that during their evolution shows a huge energy release (up to  $10^{32}$ ergs)[1]. This delivery of magnetic energy is also known as a **solar flare** and are associated with magnetic reconnection in the corona. These events can be traced in the visible range. Moreover, using the UV or longer wavelengths it is possible to retrieve information about the chromosphere where the stellar flares are taking place. All together describe the bright magnetic region at the stellar atmosphere as shown below:

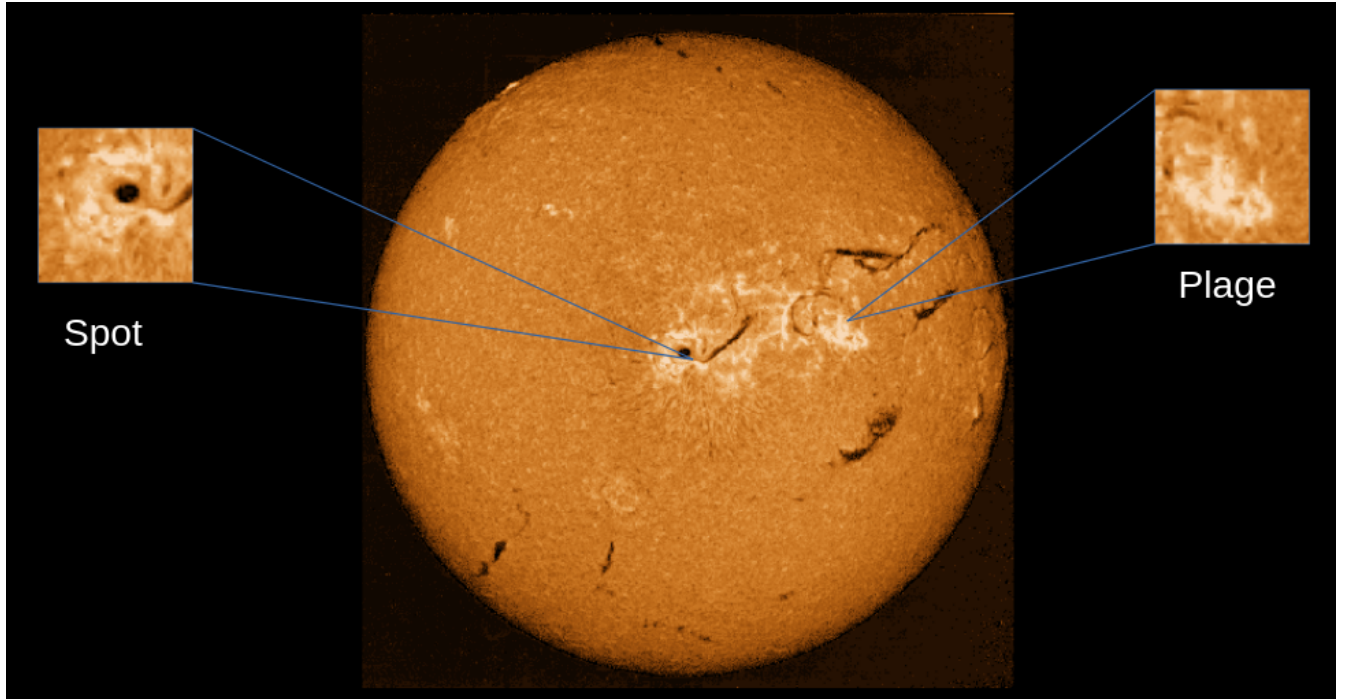


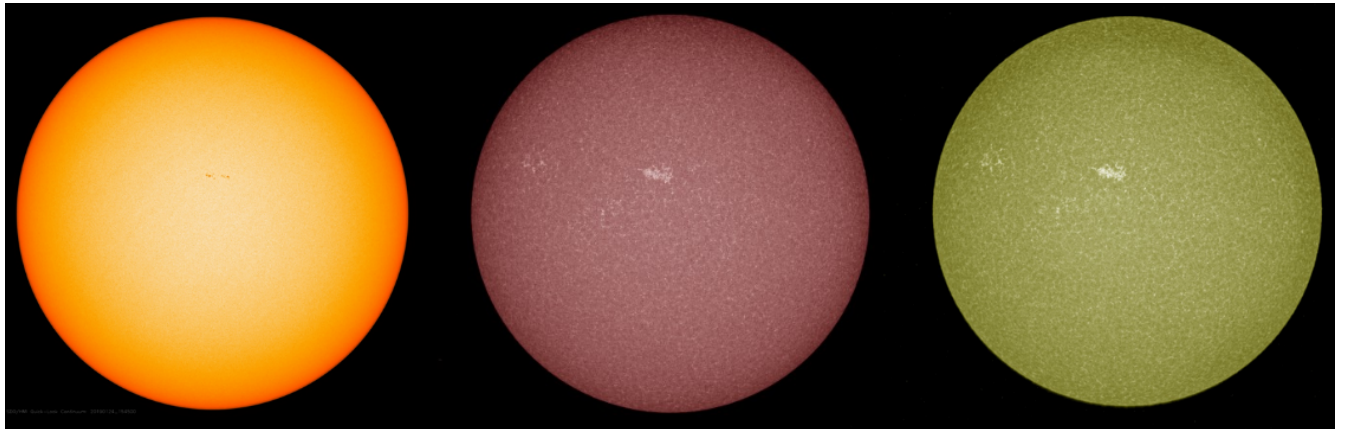
Figure 2.1: Anatomy of Sun's active region [11], is possible to observe the existance of plages without spots but not spots without plages. Also, the elongated structures observed all over the surface correspond to filaments, not sunspots.

These regions are classified as the main barriers for RV detection of Earth-like exoplanets, mainly because *faculae suppresses the underlying convection in stellar atmospheres* [1]. Taking

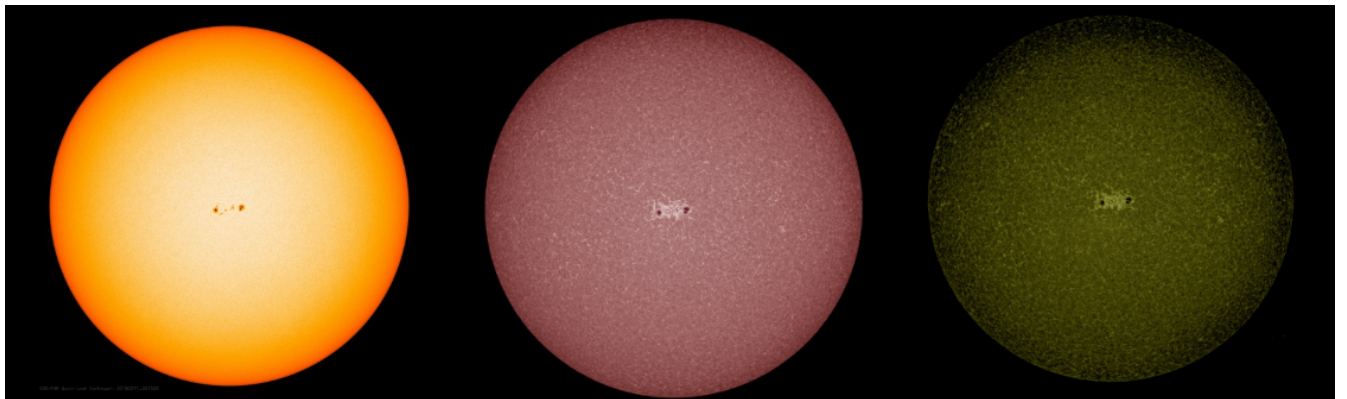
into account, that convection brings hot material from the interior, afterwards cools down and sink into the edges of intergranular lanes, producing a blushifted signal. Moreover, once faculae blocks convection in that area, the blueshift excess is modified, perturbing the RV signal.

These **Active regions** moves at the stellar surface according to Sun's rotation. When sunspots move across the solar disk, *the total amount of solar irradiance is reduced by a factor proportional to the sunspot's covering area* [2]. On the other side, when the spot is near to the limb, this total amount of energy irradiated is enhanced due to the emission of faculae. *This variability is modelled as the sum effect of the intensity deficit from sunspots and the excess from faculae and plage* [3]. Stellar observations have determined that active stars are spot-dominated, while quiet stars are more likely to be plage/faculae-dominated [4].

At the spectrum level, some stellar lines profiles have been observed to change when active regions were present (eg. Ca II produced at the chromosphere, K and Fe I at the photosphere). Such effects are explained by temperature inhomogeneities at the solar surface (hotter faculae and cooler sunspots) [6]. Another similar analysis has been made by [1], when comparing the different light curves during the transit of a solely spot and plage during a quiet sun epoch, those variations are represented by asymmetrical light-curves, which are observable in different wavelengths.



(a) Plage moving across Sun's surface. From left to right: HMI visible continuum channel, 1700 $\text{\AA}$  channel and 1600 $\text{\AA}$  channel. Images of 2019 January 14. Retrieved from SDO.



(b) Sunspot moving across Sun's surface. From left to right: HMI visible continuum channel, 1700 $\text{\AA}$  channel and 1600 $\text{\AA}$  channel. Images of 2018 February 11. Retrieved from SDO.

The size of an active region is called the **filling factor** and represents the coverage area normalised by the solar surface. The higher the parameter, the bigger the size of the active region. In this case, this factor is measured for sunspots and plage. Following the observations, the higher filling factor, the more spatially distributed, and lower contrast between plage and spots. For the case of study, -the Sun- spots and plages are not spatially coincident. Moreover, the lifetime of plages can be as long as 5 rotations whereas solar spots lifetime is usually shorter than one solar rotation, which further highlight the disconnection between both phenomena. Since, the solar disk surface is resolved (opposite to other stellar observations), it's possible to combine direct solar observations with disk-integrated spectra. Allowing us, to make a comparison between inhomogeneities on the photosphere and follow the contributions of spot/plage separately on the spectra.

## 2.1 HARPS-N

The HARPS-N is a *Echelle spectrograph that comprehends the visible range* [11]. During the day, a solar telescope linked to HARPS-N provides a near-continuous stream of disk-integrated solar spectra [5]. This instrument, observe the Sun with a daily coverage of 6hr, obtaining the solar spectrum with a resolving power  $R = 115.000$  and optical bandwidth spanning 383–690 nm. One goal of this instrument is to take spectroscopic-measurements of the Sun in order to understand how surface inhomogeneities influence the RV measurements. One proxy to quantify this anomalies is the  $\log R'_{HK}$  index, which measure the emission flux at the center of absorption lines such as  $Ca\text{ II }H\&K$ (3933 Å and 3968 Å respectively) (Figure 2.3).

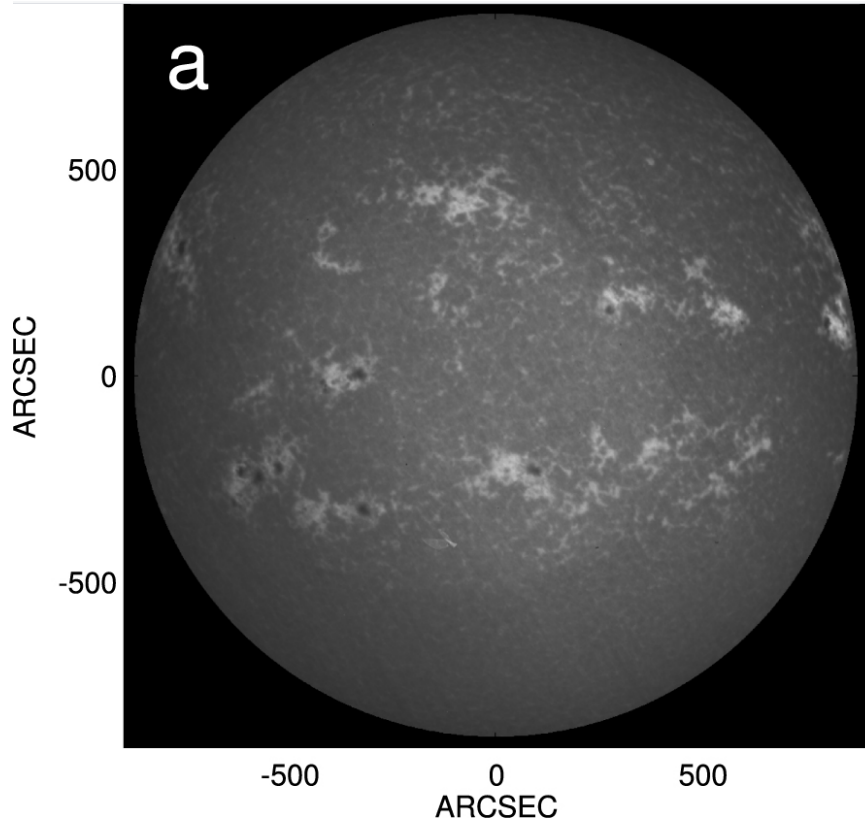


Figure 2.3: Ca II K disc centered image [15]

The CaII lines are known to correlate with the filling factor of plages [14], but this proxy is unsensitive to their location at the solar surface which must be known to better correct stellar activity in RVs [8][12][13]. Taking into account the solar cycle studied, HARPS-N is capable to observe variability even during the solar minimum registered as shown below:

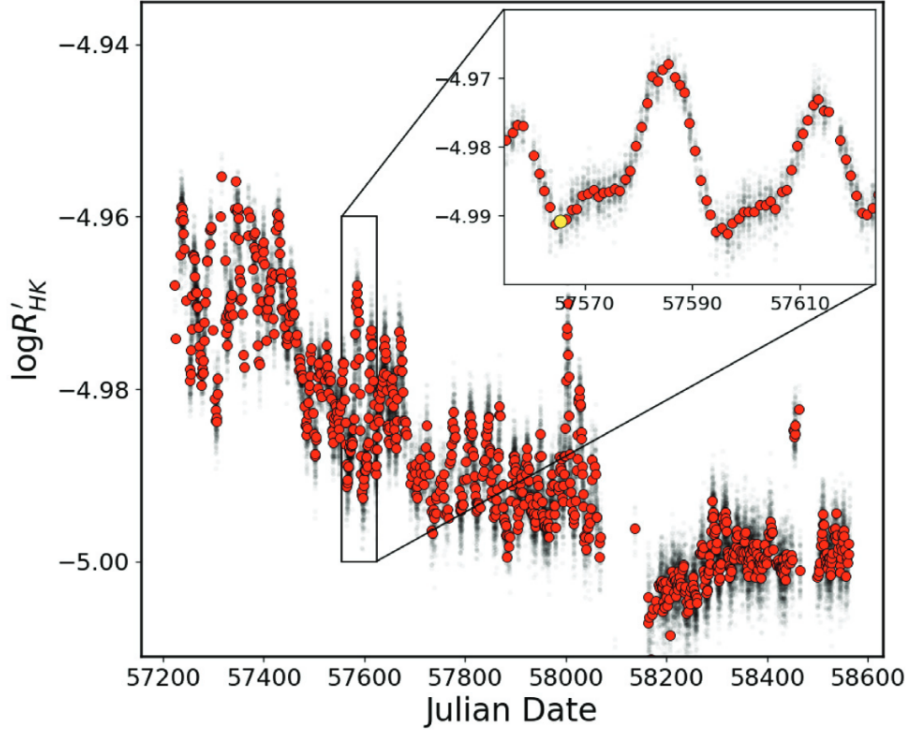


Figure 2.4: HARPS-N solar telescope  $\log R'_{HK}$  measurements of the Sun, where the variability seen is due to active regions rotating on and off the solar surface [7]

## 2.2 SDO Images

The Solar Dynamics Observatory is a program designed to understand the causes of solar variability and its impacts on Earth. The orbiter captures UV and EUV images, the cadence and duration of measurements are 1hr and 20 days. The pixel size and FOV are  $2.^{\circ}4$  and  $2048'' \times 2048''$ . The data set is composed of different wavelength bandpass (among them the  $1600\text{\AA}$  and  $1700\text{\AA}$  in the UV for instance). Those, being sensitive to the lower chromosphere and registering temperatures up to  $\log(T[K]) = 3.7$ .

# Chapter 3

## Methodology

In order to produce a full-disk map of Active Regions (**ARs**) in the Sun. It was necessary to build a dataset composed of 8309 images taken by the SDO (**Solar Dynamics Observatory**). Between January 2<sup>nd</sup> 2015 to April 4<sup>th</sup> 2022, with a minimum of one image per day. These images in the AIA-1700 and AIA-1600 filter, were selected taking into account that the strongest contributors to the plage emissions in these filters are the emissions that are produced near the temperature continuum. Furthermore, spots have a dark appearance rather than in other channels. In this way, it was possible to track the different ARs move over the surface during the 7 years of data collection as shown below:

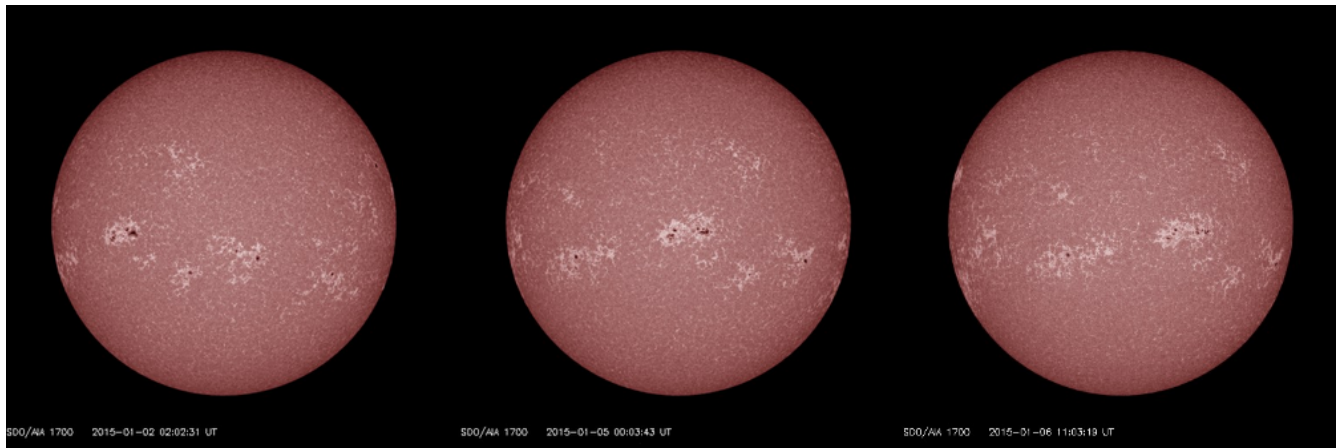


Figure 3.1: Data collection of direct Sun images from SDO in the 1700Å filter. Images taken in a time-span of 20 day during February 2018. Retrieved from SDO.

At this point, the next step was to map the occurrence of these events during time. For this purpose, we used a previous code (YAMORI, Cretignier et. al. in prep) which was able to segment all images and classify the different features observables in two different categories: **plage/spot**. With this information available, YAMORI was able to produce a table with the main important parameters for this study such as: UT date, JDB date, filling factor and position at the solar surface.

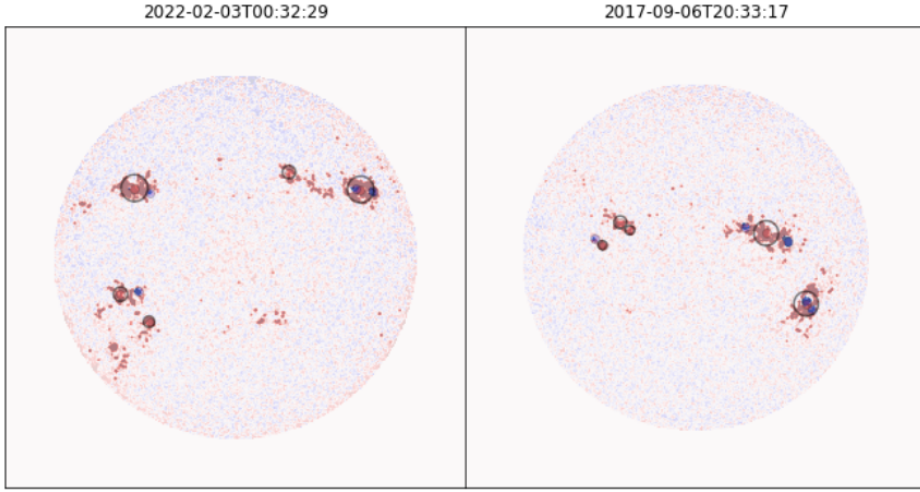


Figure 3.2: Segmentation image process from the observation with the largest active region registered in 2017 and 2022.

Subsequently, we wanted to differentiate period of times where the Sun was: **plage dominated, spot dominated and quiet Sun**.

For this, we used the filling factor to group epochs dominated by plages or spots. In Figure 3.3, we plotted the plage filling factor (%) as function of the relative spot filling factor (%). This is because, we were interested in epochs where the spots contribution was the largest as possible. Taking into account, that there can be epochs of plages without spots but not spots without plages as mentioned before.

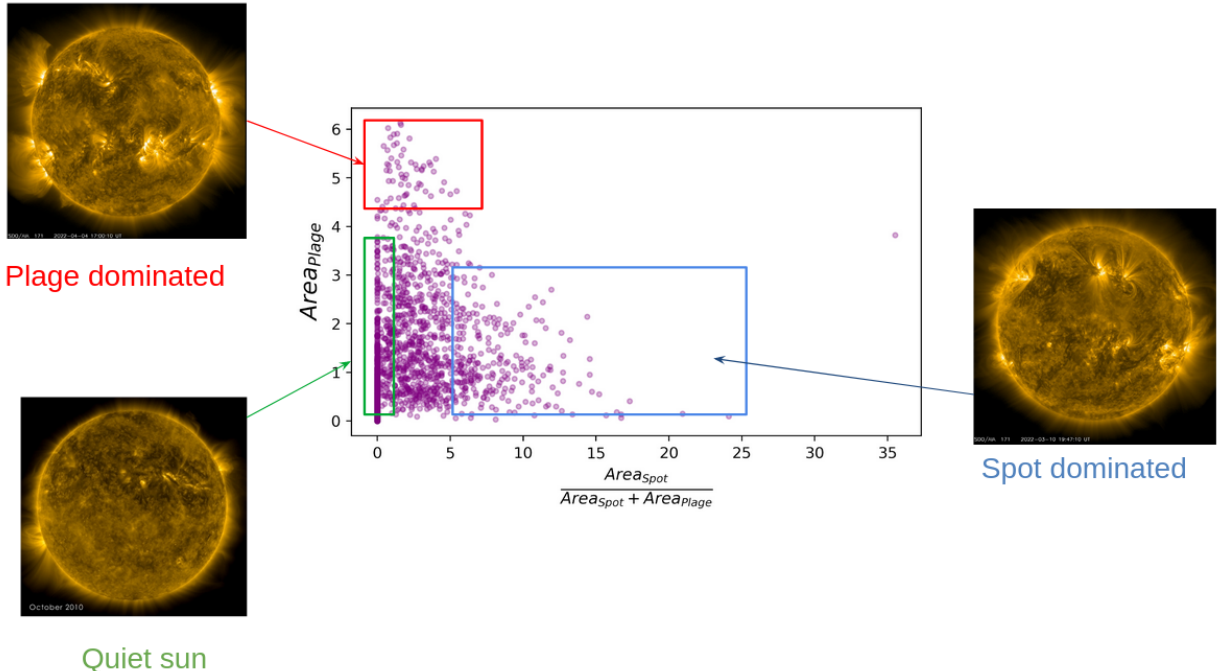


Figure 3.3: Plage filling factor (%) vs the relative spot filling factor (%). Here, the dominance regions for each feature are identified and their JDB dates retrieved respectively.

Next step, was to define sub-categories of the two main groups. The idea was to establish for each group, the location over the Sun's surface. For this, we defined three sub-regions over the surface (left, center, right). These sub-regions, were determined making a change of coordinate from  $(x,y)$  position on the image to  $(\mu,\nu)$  the “physical coordinates”. In this case, with  $\mu$  the limb angle ( $\mu=\cos(\theta)$  and  $\theta$  the angle with the vector normal to the surface) and  $\nu$  the local RV of the surface element. In this way, every sub-domain was defined in such a way that:

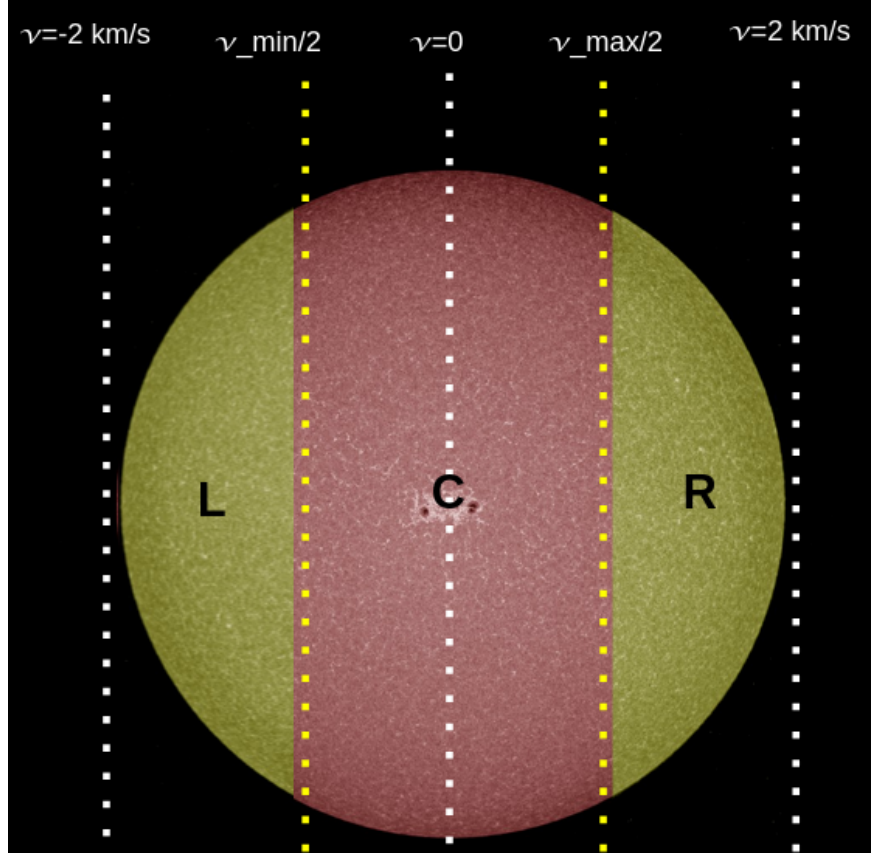


Figure 3.4: Scheme of cutoff delimitation for the three sub-regions using the physical coordinates on the image. In yellow are denoted the external areas (left-right) and in pink the central part.

We iterate this process for plage and spot respectively, in order to obtain this classification:

Dominant category	Location
Plage	Left
	Center
	Right
Spot	Left
	Center
	Right
Quiet	

We retrieved the JDB dates for each of this sub-groups. Using YAMORI, we stacked all the images for each classification, in order to verify that the cutoffs “handmade-defined” in Figure 3.3 were the best ones. When setting the cutoff values, we took care that at least 10 HARPN-S

solar spectra were existing for each sub group. Indeed, even if we have daily observations from the space SDO missions, this is not the case for the HARPS-N ground observations due to bad weather conditions as shown below :

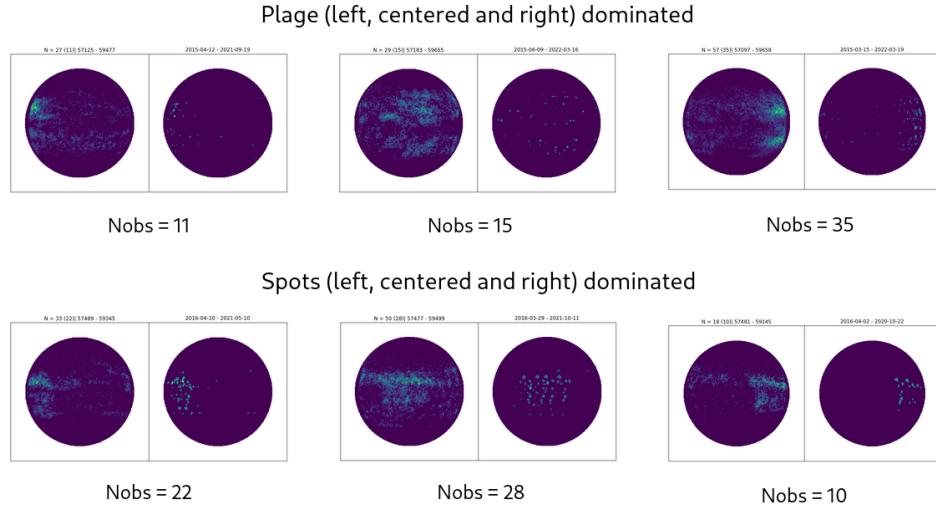


Figure 3.5: Stacked images for each sub-group with a minimum of 10 solar observation by HARPS-N. On each subplot, the left image is the stacked plage segmentation, whereas the right one is the stacked spot segmentation.

### 3.1 Left-Right area method

Once the epochs dominated by different active regions and at different stellar location were identified, we then stacked the HARPS-N corresponding spectra. In order to highlight the line profile variation, we normalised the spectra by the master quiet spectra ie. the lowest activity during the 7 years of data recording (it contains 58 observations taken mainly during the minimum solar cycle between 2018-2019).

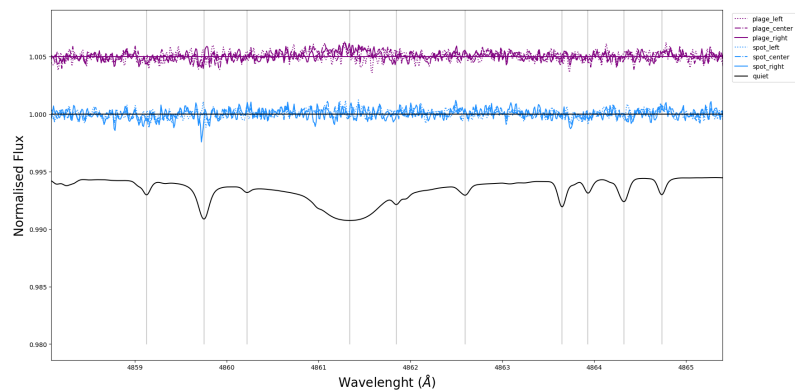


Figure 3.6: Ratio spectra produced during each region-dominance occurrence (HARPS-N) match.

To better understand the expected signature on a ratio profile, we can produce a small simulation. An active region is similar to a flux bump on a line profile that will introduce a change of sign in the ratio profile. Figure 3.7 illustrates this effect in a better way, we produced synthetic absorption lines (gaussians), one of those with a slightly shift in wavelenght, then simulating the active region line according to observations. In this case, we follow Eq. (3.1), we produced the contaminated spectra for faculae and spot such that:

$$S_{tot}(\lambda) = \frac{(1-f) \times S_q(\lambda) + f \times S_{AR}(\lambda) \times I}{(1-f) \times 1 + f \times I} \quad (3.1)$$

With  $f_{AR}$  being the filling factor ( $f_s = 0.25\%$  and  $f_p = 5\%$ ) for spot and plage and  $I_{AR}$  the intensities of ( $I_s = 33\%$  and  $I_p = 110\%$ ) respectively. In this way, when producing the ratio spectra is possible to observe the assymetry right-left mainly for faculae:

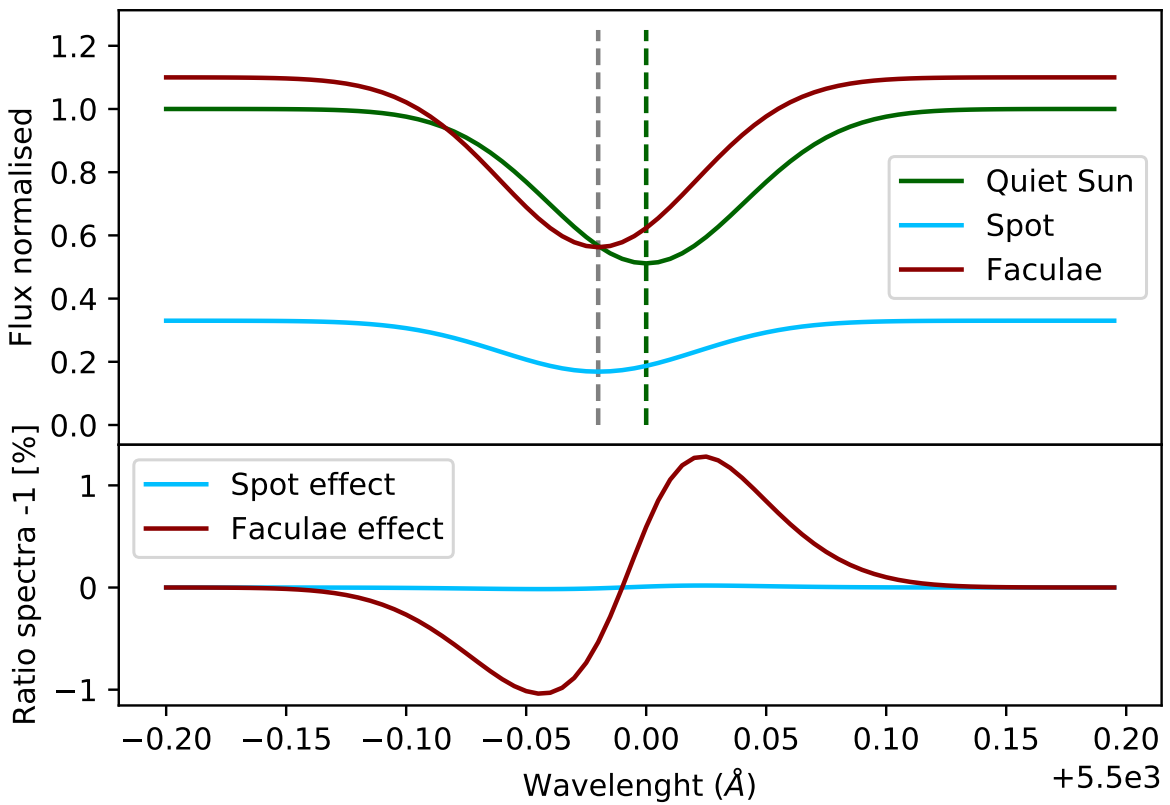


Figure 3.7: Absorption lines simulated with gaussian functions. The effect in the ratio spectra induced by each spot and faculae is observable. Mainly for faculae contributions.

In Fig.3.6, we first observe no clear signatures easily visible and the noise level is unfortunately high. It made the visual identification difficult in particular since we had to scan 2800 Å of spectra. Instead of that, we developed a mathematical metric to fit it directly on the ratio spectra for each individual line. For each stellar line, we know the line center using the Kit-Cat code [14]. This code fit a parabola on the core of the stellar lines as proxy of the wavelength center. We then integrate the area on the left side (L) and right side (R) of each stellar line with an half-window of 0.1 Å.

To quantify this asymmetry, we write a simple linear model for the left minus right area. We also fitted a linear model for a left plus right area to search for other eventual signatures such that:

$$L - R = \alpha_- \times G + \beta_- \quad (3.2)$$

$$L + R = \alpha_+ \times G + \beta_+ \quad (3.3)$$

With L - R being the integrated areas at each side and G the group variable such that:

G	Left: -1
	Center: 0
	Right: +1

In Eq [3.1] the alpha coefficient indicate an effect depending on the active region location, whereas the beta coefficient is just an offset which is only sensitive to the presence/existence of an active region (independently of its location). From the physics, we expect only an effect in  $\beta_+$  and  $\alpha_+$ . In Figure 3.7, we can see the spectra of two sub-groups specifically : plage-left and spot-left the line center is at 5232.95 Å. As we mentioned before, we were expecting to see a difference between the core lines and their different contributions, but the noise in the spectra is similar to the lines-shape even more in the case of spot contributions. The line presented here was detected by with one of the largest  $\alpha_-$  value

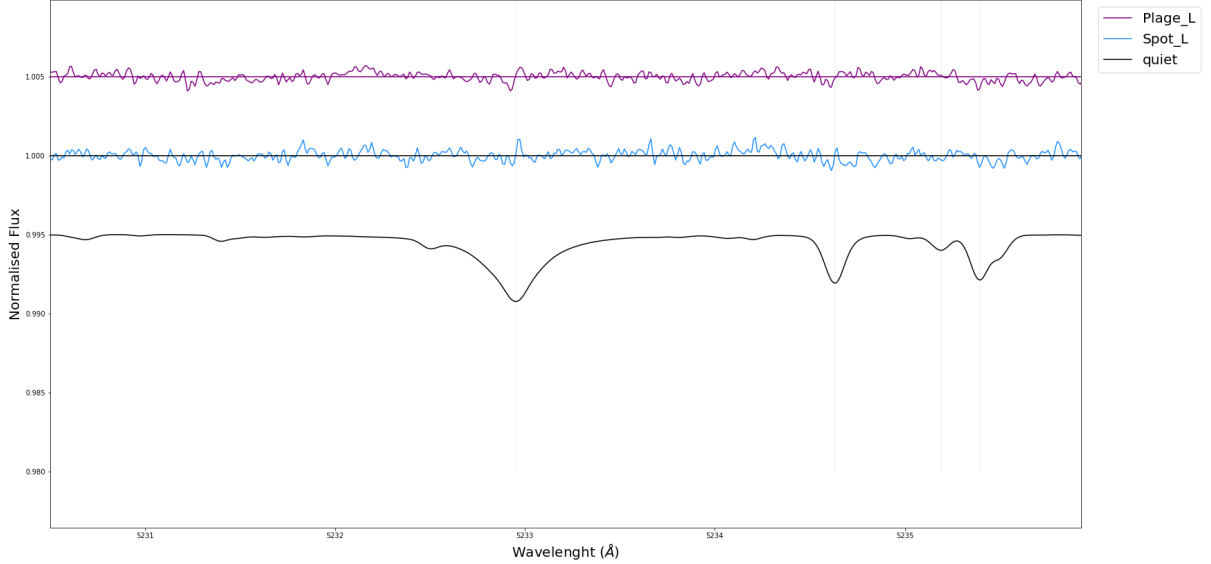


Figure 3.8: Plage-left, Spot-left and master spectra eye-comparison among their different contributions around 5233 Å line.

# Chapter 4

## Results

Initially, after measuring the corresponding filling factor mentioned before, it was possible to make a comparison between plage and spot contributions for a certain time-span. In Figure 4.1. we show how large the plage filling factor is compared to spots. The size between both active region is typically of one order of magnitude. Which is in agreement with the direct observations, but what's interesting to remark is a phase offset which could be related with other unassociated plage events over the surface:

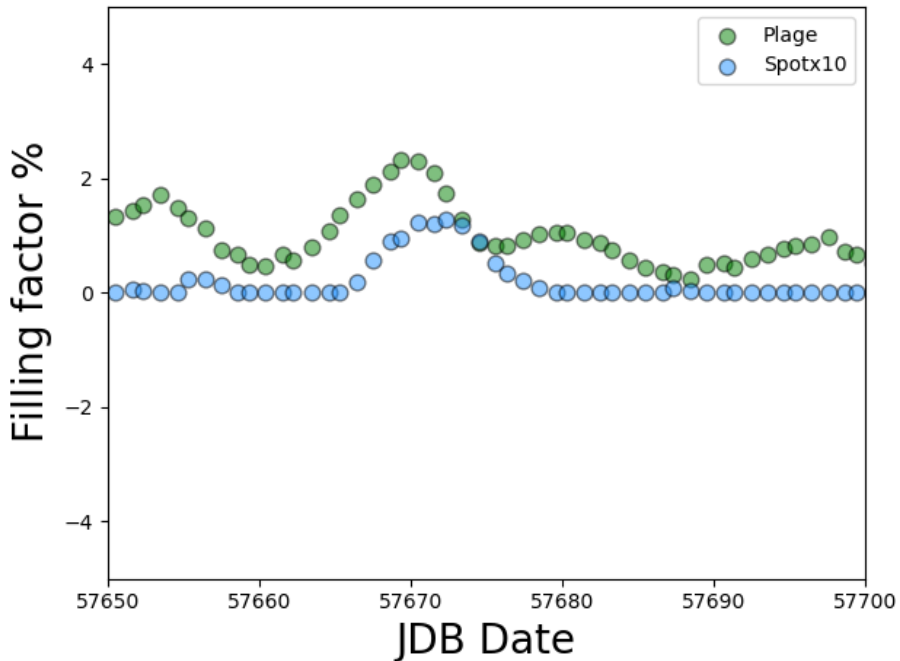


Figure 4.1: Phase shift of peak values between plage and spot contributions. As we show in Chapter I, both events are not necessarily space-related (Fig 1.1)

Furthermore, using the 4 parameters explained before, it was possible to make an analysis of the correlation between them. The idea was to find any type of outliers showing any significant difference at the line profile in the diverse spectra. Thus, indicating that the solar spectra change in a way more strongly correlated to changes in the dominant filling factor%, rather than the undominant filling factor%. Figure 4.2 shows the different relations:

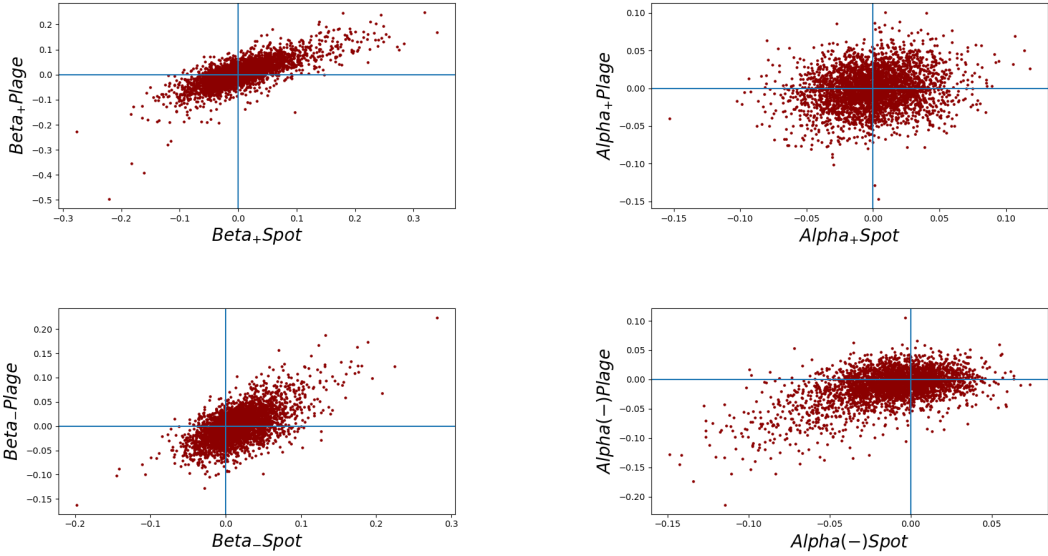


Figure 4.2: Parameter relations between  $\alpha_+$ ,  $\alpha_-$ ,  $\beta_+$ ,  $\beta_-$  for spot and plage. Each dot on this figure is a stellar line of the solar spectrum.

In this case, we observe -as expected-, outliers that are lines more sensitive to active regions. Also, nothing clearly is visible in  $\alpha_+$ , from physics we decided to focus on the  $\beta_+$  and  $\alpha_-$ . The  $\beta_+$  group is less informative since it only indicates if an active region is present, but such information are already retrieved by the  $\log(R'_{HK})$  for instance and other chromospheric proxies. Moreover, no lines seems to indicate if a spot or a plage exist and only react similarly to the presence of both of them (no outliers is detected along the crosses axes and only along the  $y=x$  line). The more remarkable group is  $\alpha_-$  which indicates a signatures depending on the stellar surface location of the active region.

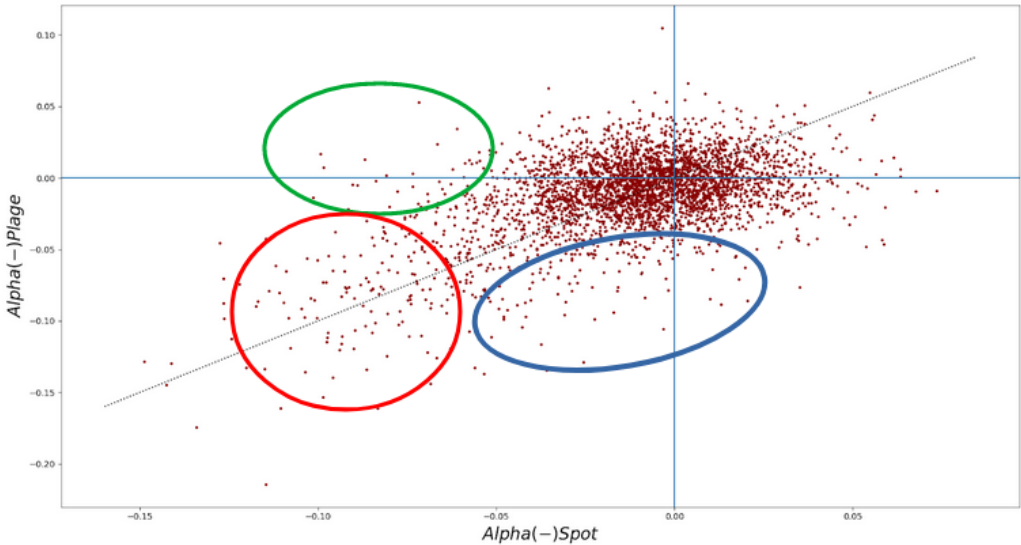


Figure 4.3: Three main groups of outliers in  $\alpha_-$  group. Each sub-division is affected at a different level by some region than the other one.

Nevertheless, to visualize it in a better way, we extract the wavelengths corresponding to this regions and subsequently we folded all lines around the line centers. In this way, it would be better to observe if any line profile was more affected according the previous explanation. Figure 4.4 shows a more detailed scheme of this process, where the folding is performed 1.5 Å around the line center as indicated by the axis of the bottom subplot. For the ratio profile, we reduce it to 0.5 Å just for visual consideration:

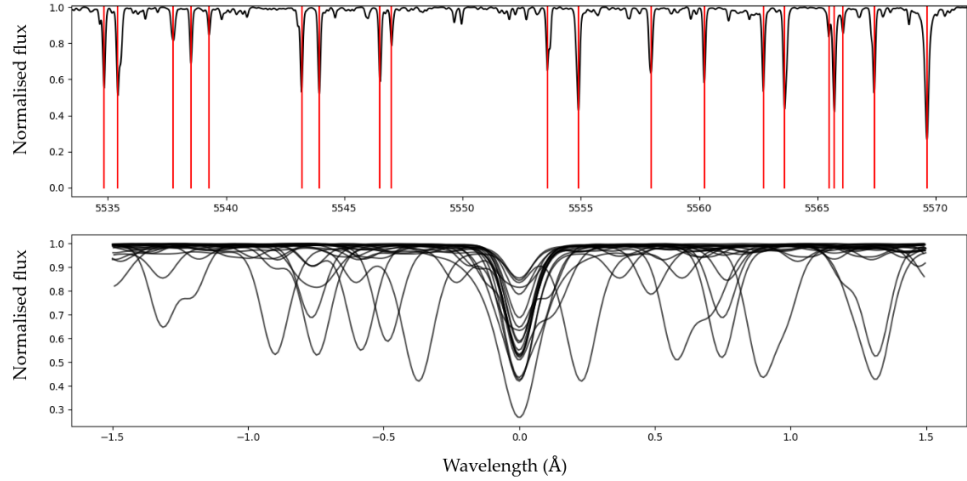


Figure 4.4: An illustration of the "line center folding" operation to cumulate the information of different stellar lines. **Top:** The initial stellar spectrum and the line list. **Bottom:** The folded representation that cumulate the information of all the lines around their line center.

We performed this process, for the three groups mentioned before. Figure 4.5 shows the folding for the more external outliers (black dots), that means a group of lines (112) that are affected by both features plage and spot. In this case, the effect of left-right difference is strongly observable as we expected following the synthetic model described before in section 3.1

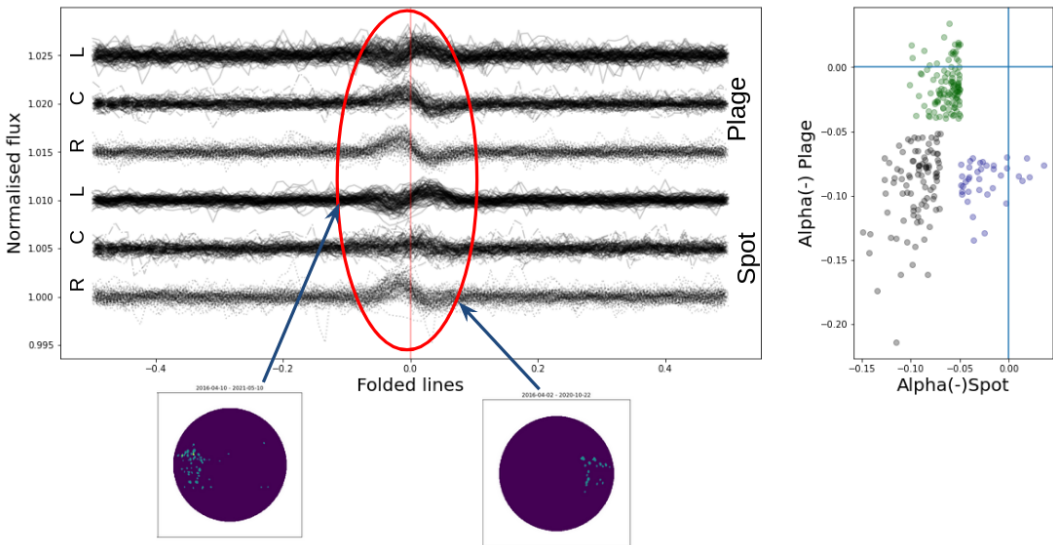


Figure 4.5: Folded ratio lines profiles corresponding to the outliers of the right subplot. L-C-R represent the lines for each surface's region (Left - Center - Right) for both events spot and plage.

On the other hand, for outliers that are getting more affected by one feature rather than the other, the effect isn't as clear as the previous example. Next Figures shows that the L-R difference is not that strong (group close to the cross axes), in some cases is almost null. This is more evident in Figure 4.7 where outliers are more affected by plage, but the spot dominated spectra is nearly flat, which is accord to the model, where the contribution of spot is minimal compared to the one from faculae.

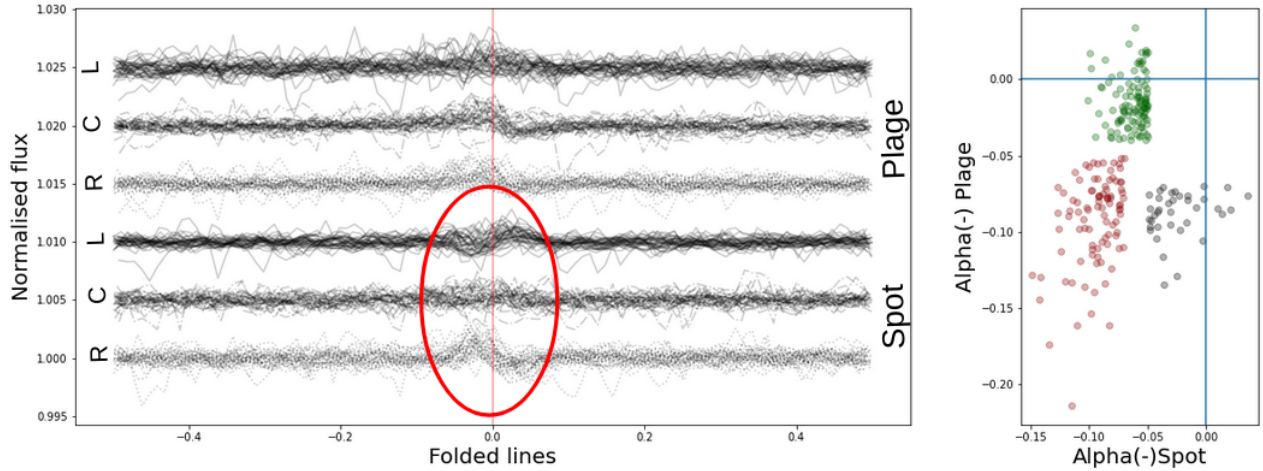


Figure 4.6: Folded lines for more Spot affected outliers.

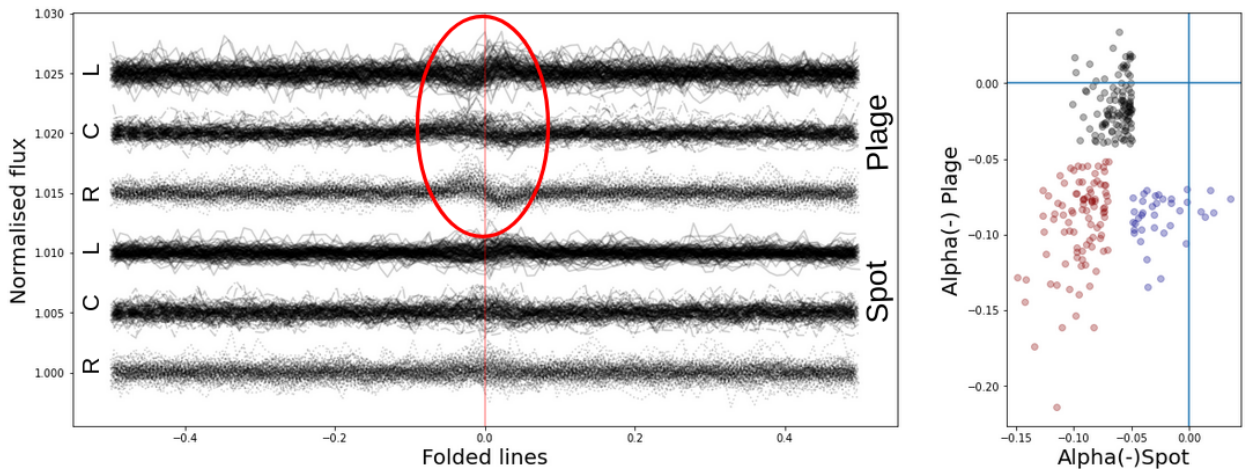


Figure 4.7: Folded lines for more plage affected outliers.

Finally, even when observing this effect, there's no clear difference between the individual contributions of each feature to the line profiles. We suggest multiple explanations that should be reviewed in the continuation of this work: For example, the difficulty to obtain clear signatures may be induced by the presence of an interference pattern on HARPS-N solar spectra [7][14]. This pattern could produce an extra source of noise, making the detection of the signatures harder whereas those latters were already difficult to be detected due to the low solar activity level. The 24 cycle being one of the least active one from a century. Also, from our simulations, the signatures of spots is at least one order of magnitude lower than the effect of faculae/plages. Those detections being already close to the precision of our data.

# Chapter 5

## Conclusions

Initially, using SDO images it was possible to map the occurrence and location of active regions during the last seven years of data collection. Using YAMORI code, it was possible to classify them as a **plage/spot** event and to measure their position at Sun's surface during their transit. From this, it was possible to know at which epochs the Sun had a dominant activity from one of the two categories and classify this activity according their location. In this way, we obtained 7 final sub-regions: (Plage[Left-Center-Right], Spot[Left-Center-Right], Quiet Sun). Also, it was possible to observe a phase shift between the peaks of plage and spot contributions, indicating that plages and spots are not purely co-spatial.

With this information, a match was made with **HARPS-N** observations in order to identify the disk-integrated spectra corresponding to plage/spot dominance. In this way, we introduced a quantitative method for measuring the change in line profiles. This method, consisted on integrate the area over the absorption line around the theoretical line center. The clear detection of a different signatures from the left and right dominated group (independently of the AR) is however a proof that we can map the location of active regions at the stellar surface even from disk-integrated spectra (more known as a **stellar surface tomography** even if here we don't know the magnetic field and the location of the AR). Something that has already been demonstrated on fast-rotating stars, but not yet on slow-rotating ones. We found three different groups of outliers. The group that was affected equally by the two categories showed a clear left-right effect. Nevertheless, for outliers getting affected more by some feature rather than the other the effect less visible.

Taking into account, that the data used in this work were taken in the context on the 24<sup>th</sup> and beginning of 25<sup>th</sup> solar cycle. The first cycle, registered its maximum value of activity with a value lower than other recent solar cycles, reaching similar quantities to those observed in cycles 12-15 (more than a hundred years ago). Finally, is possible to conclude that the sensitivity to sunspot compared to faculae is unclear due to an interference pattern produced by pseudo-features and HARPS-N systematics and because the effect expected from spots is small, whereas those latter never exist without co-existent plages that mask their signal.

# Bibliography

- [1] Toriumi, S., Airapetian, V. S., Hudson, H. S., Schrijver, C. J., Cheung, M. C., DeRosa, M. L. (2020). Sun-as-a-star Spectral Irradiance Observations of Transiting Active Regions. *The Astrophysical Journal*, 902(1), 36.
- [2] Kitai, R., Muller, R. (1984). On the relation between chromospheric and photospheric fine structure in an active region. *Solar physics*, 90(2), 303-314.
- [3] Domingo, V., Ermolli, I., Fox, P., Fröhlich, C., Haberreiter, M., Krivova, N., ... Vögler, A. (2009). Solar surface magnetism and irradiance on time scales from days to the 11-year cycle. *Space Science Reviews*, 145(3), 337-380.
- [4] Radick, R. R., Lockwood, G. W., Baliunas, S. L. (1990). Stellar activity and brightness variations: A glimpse at the Sun's history. *Science*, 247(4938), 39-44.
- [5] Dumusque, X., Glenday, A., Phillips, D. F., Buchschacher, N., Cameron, A. C., Ceconi, M., ... Walsworth, R. (2015). HARPS-N observes the Sun as a star. *The Astrophysical Journal Letters*, 814(2), L21.
- [6] Thompson, A. P. G., Watson, C. A., de Mooij, E. J. W., Jess, D. B. (2017). The changing face of Centauri B: probing plage and stellar activity in K dwarfs. *Monthly Notices of the Royal Astronomical Society: Letters*, 468(1), L16-L20.
- [7] Thompson, A. P. G., Watson, C. A., Haywood, R. D., Costes, J. C., de Mooij, E., Collier Cameron, A., ... Walsworth, R. (2020). The spectral impact of magnetic activity on disc-integrated HARPS-N solar observations: exploring new activity indicators. *Monthly Notices of the Royal Astronomical Society*, 494(3), 4279-4290.
- [8] Dumusque, X., Boisse, I., Santos, N. C. (2014). SOAP 2.0: a tool to estimate the photometric and radial velocity variations induced by stellar spots and plages. *The Astrophysical Journal*, 796(2), 132.
- [9] Boro Saikia, S., Marvin, C. J., Jeffers, S. V., Reiners, A., Cameron, R., Marsden, S. C., ... Yadav, A. P. (2018). Chromospheric activity catalogue of 4454 cool stars. Questioning the active branch of stellar activity cycles. *Astronomy and Astrophysics*, 616, A108.
- [10] Dumusque, X., Glenday, A., Phillips, D F., Buchschacher, N., Cameron, A. C., Ceconi, M., ... Walsworth, R. (2015). HARPS-N observes the Sun as a star. *The Astrophysical Journal Letters*, 814(2), L21.
- [11] University of Oregon. (s. f.). Faculae. ABYSS. Recuperado 31 de mayo de 2022, de <http://abyss.uoregon.edu/7Ejs/glossary/faculae.html>

- [12] Wilson, O. C. (1978). Chromospheric variations in main-sequence stars. *The Astrophysical Journal*, 226, 379-396.
- [13] Noyes, R. W., Hartmann, L. W., Baliunas, S., Duncan, D. K., Vaughan, A. H. (1984). Rotation, convection, and magnetic activity in lower main-sequence stars. *The Astrophysical Journal*, 279, 763-777.
- [14] Cretignier, M., Dumusque, X., Hara, N. C., Pepe, F. (2021). YARARA: Significant improvement in RV precision through post-processing of spectral time series. *Astronomy & Astrophysics*, 653, A43.
- [15] Chatterjee, S., Banerjee, D., Ravindra, B. (2016). A butterfly diagram and Carrington maps for century-long CA II K spectroheliograms from the Kodaikanal observatory. *The Astrophysical Journal*, 827(1), 87.